

## Interface traps “extrinsically” deliver MIT in monolayer MoS<sub>2</sub> FET

Nan Fang and Kosuke Nagashio

Department of Materials Engineering, The University of Tokyo

7-3-1 Hongo, Tokyo 113-8656, Japan

Phone: +81-3-5841-7161 E-mail: nan@adam.t.u-tokyo.ac.jp

### Abstract

Field-effect control of carriers are systematically studied by both  $I$ - $V$  and  $C$ - $V$  in MoS<sub>2</sub> FET. MIT origin in 2D materials is investigated. It is suggested that  $C_{it}$ -enhanced positive  $V_{TH}$  shift artificially induces the “extrinsic” MIT.

### 1. Introduction

The electrostatic field-effect control of carriers determines most of the device characteristics and needs to be fully understood before exploring the underlying physics in the electrical transport properties, for example, metal-insulator-transition (MIT) in MoS<sub>2</sub> and other 2D materials [1-3]. As for monolayer MoS<sub>2</sub>, the carrier modulation by the gate is mainly determined by the following two factors, in addition to the geometric capacitance ( $C_{ox}$ ). Intrinsically, it is limited by the quantum capacitance ( $C_Q$ ), which comes from low density of states (DOS) of MoS<sub>2</sub> and Fermi-Dirac distribution. Extrinsically, it is also severely affected by the interface trap capacitance ( $C_{it} = e^2 D_{it}$ ). Therefore, by intensively investigating the high- $k$ /MoS<sub>2</sub> FET with  $C$ - $V$  measurement so far, we have elucidated all the constituents of the total capacitance ( $1/C_{total} = 1/C_{ox} + 1/(C_Q + C_{it})$ ) [4].

In this study, on the basis of well extracted  $C_Q$  and  $C_{it}$ , we first reproduce MIT in  $I$ - $V$  characteristics by utilizing the drift current model. Then, through this modeling, we would like to indicate that the origin of MIT is external outcome resulting from  $C_{it}$ .

### 2. Experiments

Monolayer MoS<sub>2</sub> films are mechanically exfoliated on insulating quartz substrate from natural bulk MoS<sub>2</sub> flakes. Ni/Au was deposited as source/drain electrodes. Then, 1-nm Y metal was deposited via thermal evaporation of the

Y metal in a PBN crucible at an Ar atmosphere with a partial pressure of  $10^{-1}$  Pa, followed by oxidization at atmosphere to form buffer layer. 10-nm Al<sub>2</sub>O<sub>3</sub> oxide layer was deposited by atomic layer deposition. The Raman measurement was employed for determining the layer number. The electrical measurements were performed in the vacuum prober. Alternatively, the back-gate four-probe FET with monolayer MoS<sub>2</sub> on 90-nm SiO<sub>2</sub>/ $n^+$ -Si substrate is prepared for MIT study.

### 3. Quantum capacitance in monolayer MoS<sub>2</sub>

Fig. 1 shows the schematic drawing and the optical image of top-gate monolayer MoS<sub>2</sub> FET on quartz substrate for  $C$ - $V$  measurement. Quartz substrate was used to totally suppress parasitic capacitance. Films with large area ( $>30 \mu\text{m}^2$ ) were selected for device fabrication and characterization.  $C_Q$  was originally derived from partially screening in 2D electron gas [5]. As for monolayer MoS<sub>2</sub>,  $C_Q$  originates from partially occupied density of states (DOS) of

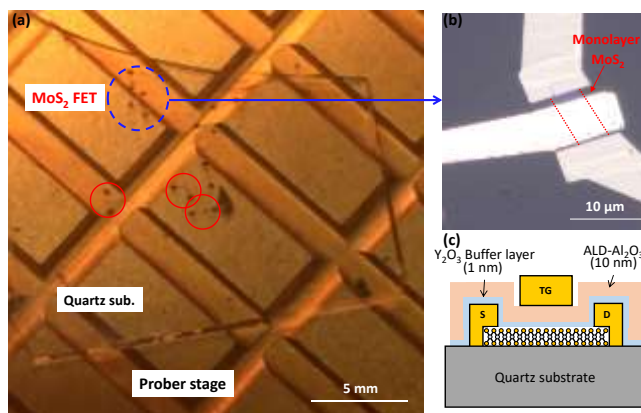


Fig. 1 (a,b) Optical image and (c) schematic diagram of top-gate monolayer MoS<sub>2</sub> FET.

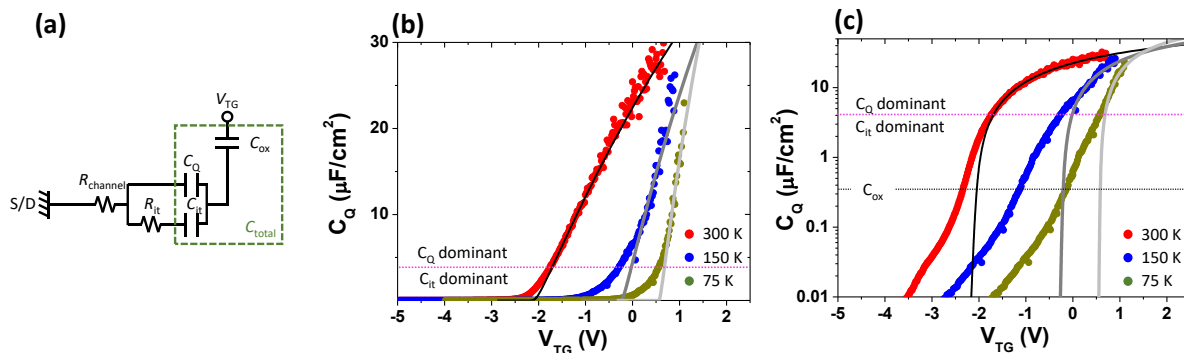
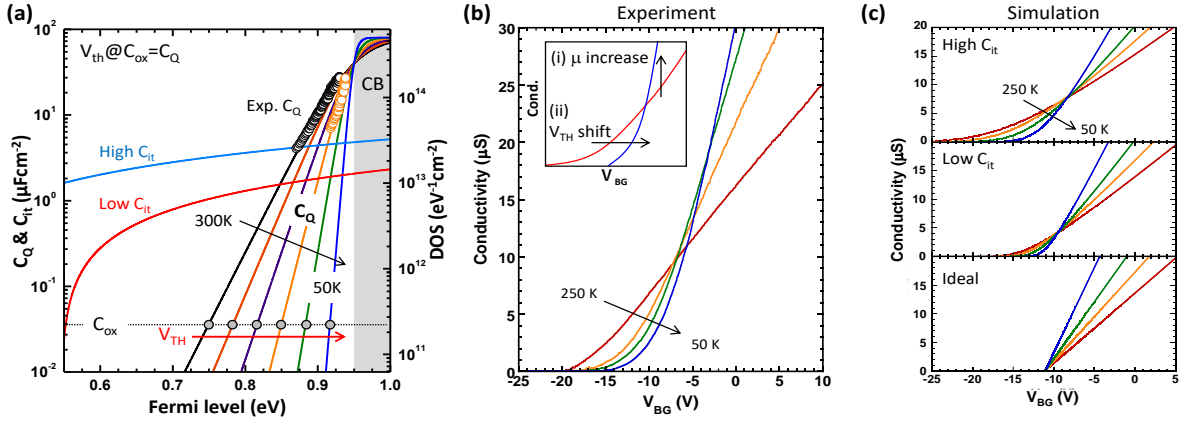


Fig. 2 (a) Equivalent circuit of  $C$ - $V$  measurement in MoS<sub>2</sub> FET. (b)  $C_Q$  extracted as a function of  $V_{TG}$  at 300 K, 150 K and 75 K. Solid lines are the theoretical fitting curves. (c) The same figure as (b) with the logarithmic scale.



**Fig. 3** (a)  $C_{it}$  and  $C_Q$  extracted and calculated at different temperatures (300 & 150 K for exp.). High and low  $C_{it}$  lines are used for the simulation. (b) Experimental 4P conductivity as a function of  $V_{BG}$  at 50~250 K. (c) Simulated  $\sigma$ - $V_{BG}$  curves with different  $C_{it}$  levels.

CB modulated by Fermi energy ( $E_F$ ) in Fermi-Dirac distribution. Here,  $C_Q$  is experimentally extracted from capacitance between source/drain and top-gate. The simplified circuit is shown in **Fig. 2a**. By neglecting the access resistance effect at accumulation region and extracting  $C_{ox}$ ,  $C_Q$  and  $C_{it}$  can be extracted. **Fig. 2b, c** shows experimentally extracted  $C_Q$  from  $C$ - $V$  at 1 MHz for temperature range of 75~300 K. The extracted  $C_Q$ - $V_{TG}$  curves are divided into two regions. The first region is the  $C_Q$  dominant region, with  $C_Q > C_{it}$ . In this region,  $C_Q$  has a clear temperature dependence and fits well with the theoretical calculation. The slope of  $C_Q$  becomes sharp at low temperatures due to the intrinsic nature of the Fermi distribution, which provides an alternative means to confirm the validity of  $C_Q$  extraction. The other region is the  $C_{it}$  dominant region, with  $C_Q < C_{it}$ . The  $C_Q$ - $V_{TG}$  curve deviates from theoretical curve and shows a gradual change with decreasing temperature.

#### 4. MIT origin in monolayer MoS<sub>2</sub>

Having confirmed  $C_Q$ , carrier density in the CB can be directly estimated. Drift current model is then used to simulate carriers transport process, which enables us to correlate  $I$ - $V$  with  $C$ - $V$ .  $C_{it}$  degrades the field-effect control of carriers through following equation.

$$V_{T/BG} = V_{T/BG, mid-gap} + \int_0^{E_F/e} (C_Q + C_{it} + C_{ox}) / C_{ox} d(E_F / e) \quad (1)$$

MIT is often observed in 2D materials as cross-over point in  $I$ - $V$  for different temperatures. This  $I$ - $V$  curve is reproduced by above simulation. **Fig. 3a** shows  $C_Q$  and  $C_{it}$  in the monolayer MoS<sub>2</sub> FETs for different temperatures. **Fig. 3b** shows experimental conductivity ( $\sigma$ )- $V_{BG}$  characteristics from four-probe back-gate device, which clearly shows MIT. Experimental  $\sigma$ - $V_{BG}$  characteristics is simulated with three different  $C_{it}$  levels (high, low and no  $C_{it}$ ) and plotted in **Fig. 3c**.

MIT can be observed intuitively by the combination of (i) the increase in the mobility and (ii) positive  $V_{TH}$  shift with decreasing the temperature. Within the present model,

the mobility is assumed to increase with decreasing temperature due to suppression of phonon scattering. Therefore, the dominant key factor for MIT is a positive  $V_{TH}$  shift with decreasing temperature. This occurs because  $E_F$  at  $V_{TH}$  approaches the conduction band edge at lower temperature since  $V_{TH}$  is defined by  $V_{BG}$  at  $C_Q = C_{ox}$ , which is shown in **Fig. 3a**. Thus, a larger amount of  $C_{it}$  needs to be filled by electrons before reaching  $V_{TH}$  at lower temperature, resulting in the  $V_{TH}$  shift. By decreasing the  $C_{it}$  level, the cross-over points of the MIT (shown by arrow in **Fig. 3c**) get close to  $V_{TH}$  and finally enter the subthreshold region for the case with no  $C_{it}$ , which is the ideal  $V_{TH}$  shift.

Recently, no MIT has been reported for an  $h$ -BN-encapsulated monolayer CVD-MoS<sub>2</sub> FET, suggesting a quite low  $C_{it}$  due to superior 2D/2D interface properties [6]. It should be noted that ultra-thin 2D materials with reduced DOS is more sensitive to the interface disorder, since the carrier modulation is controlled by the relative magnitude of  $C_Q$  and  $C_{it}$ . The present model indicates that  $C_{it}$ -enhanced positive  $V_{TH}$  shift is one of the main origins for “extrinsic” MIT. Cross-over point in  $I$ - $V$  is just the outcome of carrier band transport under degraded field-effect modulation for different temperatures.

#### 5. Conclusions

Field-effect control of carriers were systematically studied by both  $I$ - $V$  and  $C$ - $V$  in monolayer MoS<sub>2</sub> FET.  $C_{it}$ -enhanced positive  $V_{TH}$  shift is suggested to be one of the main origins for “extrinsic” MIT.

#### Acknowledgements

NF was financially supported by JSPS KAKENHI. This research was partly supported by the JSPS Core-to-Core Program, A. Advanced Research Networks, JSPS KAKENHI Grant Numbers JP16H04343, Japan.

#### References

- [1] B. Radisavljevic *et al.*, Nature Materials 2013, **12**, 815. [2] X. Chen X *et al.*, Nature Commun. 2015, **6**, 6088. [3] Z. Yu *et al.*, Nature Commun. 2014, **5**, 5290 [4] N. Fang *et al.*, J. Phys. D 2018, **51**, 065110. [5] S. Luryi, Appl. Phys. Lett. 1988, **52**, 501. [6] X. Cui *et al.*, Nature Nanotech. 2015, **10**, 534.